frontiers | Frontiers in Marine Science

TYPE Original Research
PUBLISHED 19 June 2024
DOI 10.3389/fmars.2024.1380801

OPEN ACCESS

EDITED BY
Andrew Stanley Mount,
Clemson University, United States

REVIEWED BY
Songlin Liu,
Chinese Academy of Sciences (CAS), China
José Q. García-Maldonado,
Cinvestav Unidad Mérida, Mexico

*CORRESPONDENCE
Yongze Xing
xingyongze@4io.org.cn
Tiezhu Mi
mitiezhu@ouc.edu.cn

RECEIVED 02 February 2024
ACCEPTED 04 June 2024
PUBLISHED 19 June 2024

CITATION
Wang Z, Zheng P, Xing Y, Mi T and Zhen Y (2024) Archaeal communities in natural and artificially restored mangrove sediments in Tieshan Bay, China.
Front. Mar. Sci. 11:1380801.
doi: 10.3389/fmars.2024.1380801

Archaeal communities in natural and artificially restored mangrove sediments in Tieshan Bay, China

Zixiang Wang[1,2], Pengfei Zheng[1], Yongze Xing[1]*, Tiezhu Mi[2,3,4]* and Yu Zhen[2,3,4]

[1]Key Laboratory of Tropical Marine Ecosystem and Bioresource, Fourth Institute of Oceanography, Ministry of Natural Resources (MNR), Beihai, China, [2]Key Laboratory of Marine Environment and Ecology, Ministry of Education, College of Environmental Science and Engineering, Ocean University of China, Qingdao, China, [3]Laboratory for Marine Ecology and Environmental Science, Pilot National Laboratory for Marine Science and Technology (Qingdao), Qingdao, China, [4]Frontiers Science Center for Deep Ocean Multispheres and Earth System, Ocean University of China, Qingdao, China

Mangrove forests are crucial wetland ecosystems located in tropical and subtropical intertidal zones, but they have become extensively degraded. As a viable ecological restoration strategy, the cultivation of native mangrove vegetation in these degraded areas has gained considerable attention. Mangroves' unique environmental conditions make them suitable habitats for diverse microbial communities, including Archaea - one of the main microbial communities in mangrove sediments - which plays a pivotal role in biogeochemical cycles. However, little is known about the dynamics of archaeal communities during mangrove restoration through phytoremediation. In this study, we investigated the physicochemical properties of sediment profiles from natural and artificially restored mangrove ecosystems in Tieshan Bay. We utilized quantitative polymerase chain reaction (qPCR) and 16S rRNA gene sequencing techniques to explore differences in abundance, community structure, and composition of archaeal communities between sediment profiles in natural and artificially restored mangrove ecosystems. We also examined correlations between archaeal communities and environmental factors. Our results revealed that Crenarchaeota, Thermoplasmatota, Asgardarchaeota, Nanoarchaeota, and Euryarchaeota were the predominant archaeal phyla, with significant variation in sediment composition observed for Crenarchaeota and Thermoplasmatota in different depths. We also found significant differences in archaeal abundance and community composition between natural and restored mangrove sediments. Furthermore, C/N ratio and pH emerged as primary drivers of archaeal communities in wet and dry season sediments, respectively. Additionally, the study revealed seasonal disparities in seasonal differences in the relative abundance of certain archaeal groups (such as Asgardarchaeota, Nanoarchaeota). Network analysis demonstrated stronger interconnections among archaeal communities in sediments from natural mangroves than from artificially restored ones. These findings enhance our knowledge of archaeal community succession patterns in mangrove restoration, as well as provide fresh perspectives for the sustainable management of mangrove ecosystems.

KEYWORDS

archaeal community, mangroves, restored, depth, co-occurrence network

1 Introduction

Mangroves are essential wetland ecosystems that dominate the intertidal zone in subtropical and tropical coastal regions (Reef et al., 2010; Alongi, 2015; Friess et al., 2019), spanning approximately 145,068 km^2 in 2020 globally (Jia et al., 2023). These ecosystems provide a wide range of valuable ecological services, including food and raw materials, protection against waves and wind, water purification, erosion control, maintenance of fisheries, and carbon sequestration (Barbier et al., 2011). However, the world's mangrove forest area has experienced a steady decline of 3×10^3 km^2 annually from the 1980s to 2000s and an average annual loss of 0.13% between 2000 and 2016 (Valiela et al., 2001; Goldberg et al., 2020). The degradation and loss of vegetation have a substantial and adverse impact on soil multifunctionality, subsequently ensuing soil erosion significantly modifies soil properties (Hu et al., 2024). To raise awareness of the importance of these invaluable ecosystems, a flurry of international conservation policies and strategies has been introduced (Buelow et al., 2022). Cultivating mangroves is an eco-friendly method of restoring this ecosystem (Tran et al., 2019). Researchers have found that mangrove restoration increases the levels of surface sediment nutrient contents (e.g., TC, TN, and C/N) but decreases the pH values, with nutrient contents increasing and pH decreasing gradually as restoration ages (Mishra et al., 2003; Huang et al., 2022; Sun et al., 2024).

In mangrove ecosystems, specific environmental conditions render mangroves as hotspots for microbial diversity. The resident microbes play a crucial role in the material cycle and energy flow of the mangrove ecosystem (Holguin et al., 2001). Archaea, being one of the most important microbial communities extensively distributed in mangrove sediments (Zhang et al., 2021), can play a critical role in the C, N, and S cycles within the biogeochemical cycle, such as carbon assimilation, nitrogen fixation, and sulfide oxidation (Offre et al., 2013). The development of molecular biology techniques has enabled the comprehensive exploration of microbial communities, revealing a high diversity and range of metabolisms inhabiting mangroves (Zhang et al., 2021). Previous studies have demonstrated that mangrove restoration significantly influences microbial communities, and the ecological state after ten years is comparable to that of native mangroves (Lin et al., 2021). Seasonal variations have been shown to exert significant influences on the community diversity, composition, and abundance of archaea (Wang et al., 2013; Zhou et al., 2017; Liu et al., 2021). Meanwhile, the layered distribution of archaea in mangrove sediments has been reported in relation to the community structure across different depths (Otero et al., 2014; Luis et al., 2019). Zhou et al. (2017) discovered distinct stratified distribution patterns in the abundance and composition of both bacteria and archaea, potentially modulated by the availability of oxygen and gradient distribution of terminal electron acceptors along the depth profile. Furthermore, numerous studies have examined the impact of influential environmental factors such as pH, salinity, total nitrogen, total phosphorus, and organic matter on the archaeal community (Zhou et al., 2017; Zhang et al., 2018; Zhao et al., 2020). Although the understanding of microbial community and the role of microbes have been widely investigated in various mangrove environments around the world, to the best of our knowledge, little research has been conducted in Tieshan Bay, let alone investigations on the effects of mangrove restoration, sediment depth on archaeal community changes.

We hypothesized that mangrove restoration alters the abundance, diversity, composition, and structure of sediment archaeal communities. Additionally, we anticipated that sediment environmental factors influence these communities, with distinct key factors driving the season- and depth-induced distributions of archaeal communities. To test these hypotheses, we identified the main environmental factors and employed real-time PCR (qPCR) and high-throughput sequencing of the 16S rRNA gene. Our objectives were: (i) To explore the impact of mangrove restoration on the abundance, diversity, composition, and community structure of sediment archaea; (ii) To examine the vertical distribution and seasonal dynamics of archaeal communities in mangrove sediments; (iii) To identify the main sediment environmental factors affecting the structure of archaeal communities and their seasonal correlations.

2 Materials and methods

2.1 Study area and sample collection

Tieshan Bay, a semi-enclosed bay located in the northeast of Beibu Gulf (21°26′–21°40′N, 109°15′–109°45′E), has a coastline of 170 km and a bay area of 340 km^2. It is one of the main distribution areas of mangroves in Guangxi. The sampling sites have a subtropical monsoon climate, with an annual average temperature of 22.6°C and a precipitation of 1663.7 mm (http://www.bhtsg.gov.cn/zjgq/qwzs/t14741656.shtml). Influenced by the East Asian monsoon, the year can be divided into two main periods: April to October, characterized by a wet season, and November to March, characterized by a dry season (Chen et al., 2009). Since 2018, coastal engineering has led to the coverage of kaolin on some mangroves in Tieshan Bay, altering the substrate environment and causing the widespread death of mangroves in the area. In 2020, the local government repaired the damaged mangroves, implementing a restoration plan that involved removing dead mangrove vegetation and replanting local species such as *Rhizophora stylosa* Griff. and *Avicennia marina*.

In this study, natural mangroves (NM) that were not affected by coastal engineering (109°36′36″ E, 21°36′2″ N) and artificially restored mangroves (ARM) (109°36′47″ E, 21°36′3″ N) were selected as sampling sites (Figure 1). The main tree species in the ARM and NM regions are primarily *Avicennia marina*, with a small distribution of *Rhizophora stylosa* Griff. In order to eliminate the influence of tree species, this study conducted sampling all in the sediments of *Avicennia marina*. In November (dry season) 2021 and May (wet season) 2022, sediments were collected at a depth of approximately 30 cm in NM and ARM, respectively. The sediment samples were strictly segmented into 5 cm increments on site, resulting in sediment samples of 0–5 cm, 5–10 cm, 10–15 cm, and 15–20 cm. Three nearby 5×5 m quadrats were randomly selected

from each of the two sampling stations, resulting in a total of 48 sediment samples (2 sites × 4 layers × 2 seasons × 3 replicates) collected. The average of three replicate samples was displayed in the subsequent analysis results. After the samples were packed in sterile sealing bags, they were immediately transported back to the laboratory. All samples were divided into two parts: one part was stored at 4°C for physicochemical analysis, while the other part was stored at -80°C for DNA extraction.

2.2 Environmental factors determination

In the laboratory, sediment pH and salinity were determined in a sediment suspension consisting of 2 g of dried sediments (sediment-to-water ratios were 1:2.5 and 1:5, respectively) utilizing a multiparameter water analyzer (Thermal A329, USA) as described in previous studies (Huang et al., 2008). Sediment samples were dried at 60°C for 48 hours in a hot air oven and then determined for total organic carbon (TOC) using the wet oxidation method (Fernandes et al., 2022). Total carbon (TC) and total nitrogen (TN) were analyzed by an elemental analyzer (Li et al., 2019; Li et al., 2021). Total phosphorus (TP) was determined utilizing the ammonium molybdate spectrophotometric method (Huang et al., 2022). C/N was obtained by converting the units of TC and TN concentration to mol·kg^{-1} and then calculating the ratio (Hu et al., 2022).

2.3 DNA extraction and determination of the archaeal abundance by qPCR

Genomic DNA from all sediment samples was extracted using CTAB method (Cho et al., 1996). After DNA was extracted, 1% agarose gel electrophoresis was applied to check the concentration and purity. Primer pair Arch524F (5′-TGYCAGCCGCCG CGGTAA-3′)/Arch958R (5′-YCCGGCGTTGAMTCCAATT-3′) was used to quantify the abundance of archaeal 16S rRNA gene through qPCR (Li et al., 2022). SYBR Green qPCR was performed using a Roche LightCycler® 480 II, 384 qPCR instrument (Roche, Switzerland). The qPCR system contained 2× SYBR real-time Green PCR premixture (10 μL), 0.4 μL forward and reverse primers (10 μM), and 1 μL DNA template that was 10-fold diluted from 10^1 to 10^7. The qPCR conditions were as follows: 95°C for 5 min, followed by 40 cycles of denaturation at 95°C for 15 s, annealing and extension 60°C for 30 s. Standard curves were established based on the gradient concentration and target 16S rRNA gene, yielding an amplification coefficient (r^2) of 0.997 and an efficiency of 94.54%, respectively.

2.4 16S rRNA gene Illumina sequencing and bioinformatics analysis

Polymerase chain reaction (PCR) was used to amplify the V4–V5 high variable regions of archaea 16S rRNA gene, with primer Arch519F (5′-CAGCCGVVGVGGTAA-3′)/Arch915R (5′-GTGCT CCCCCGC CAATTCCT-3′) (Coolen et al., 2004; Li et al., 2019). PCR reactions were performed using 15 μL of Phusion® High-Fidelity PCR Master Mix (New England Biolabs), 2 μM of forward and reverse primers, and approximately 10 ng template DNA. The thermal cycling consisted of an initial denaturation at 98°C for 1 min, followed by 30 cycles of denaturation at 98°C for 10 s, annealing at 50°C for 30 s, and elongation at 72°C for 30 s. A final elongation step was conducted at 72°C for 5 min. PCR products were detected by 2% agarose gel electrophoresis and purified using Universal DNA purification kit (TianGen, China). Illumina NovaSeq high-throughput sequencing was used to accomplish paired-end sequencing. The high-throughput sequencing data were demultiplexed by barcode to obtain valid sequences using QIIME 2 (v.2019.1) (Bolyen et al., 2019). The DADA2 (Callahan et al., 2016) plugin in QIIME 2 was applied to perform quality control, denoising, trimming, and chimerism removal on the original sequences of all sediment samples to generate amplicon variants (ASVs) table. ASVs can be considered as 100% operational taxonomic units (OTUs) (Mescioglu et al., 2019). To accomplish taxonomic assignment, DADA2 was utilized to match ASVs against the Silva rRNA v138 database serving as reference (Pruesse et al., 2012) and taxonomy confidence threshold value of 70%. Alpha

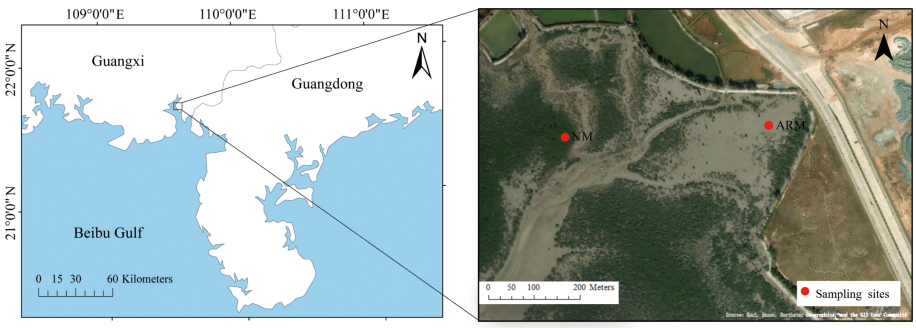

FIGURE 1
Sampling sites of artificially restored mangroves (ARM) and natural mangroves (NM).

diversity including observed ASVs, Shannon, Chao1 index and coverage was calculated using the diversity plugin of QIIME 2.

2.5 Statistical analysis

The effects of different seasons and sites on physicochemical properties and archaea communities were analyzed using *t*-test. One-way analysis of variance (ANOVA) was conducted to evaluate the impact of different depths on sediment property and archaea. A significance level of $P < 0.05$ was considered statistically significant. The archaea structure of all sediment samples was examined through Nonmetric multidimensional scaling (NMDS) ordination based on Bray-Curtis distance utilizing vegan package (Dixon, 2003) in R v4.2.3. Analysis of similarities (ANOSIM) analysis was performed using the "anosim" function from the vegan package based on the Bray-Curtis distance, respectively, algorithm with 999 permutations used for the permutation tests. STAMP v2.1.3 (Parks et al., 2014) was used to assess the statistically significant differences in the relative abundance of archaeal at the phylum, class, and genus levels in different sites and seasons. Redundancy analysis (RDA) and Pearson correlation analysis were conducted to elucidate the relationships between the archaea communities and environmental factors. Microbial co-occurrence networks from sequencing data commonly identify community member interactions (Berry and Widder, 2014). Spearman correlation coefficients were computed for the ASVs with relative abundance exceeding 0.05%, which were chosen for network analysis. Only significant correlation (correlations coefficient $|p| > 0.6$, and $P < 0.01$) were retained for constructing the network (Lu et al., 2022). The igraph package (Hartvigsen, 2011) was used to derive the files of edges and nodes for constructing the co-occurrence network, which was subsequently visualized by importing the files into Gephi v0.9.2 (Jacomy et al., 2014). PICRUSt was developed for prediction of functions from 16S marker sequences, and has become widely adopted (Douglas et al., 2020). In this study, functional prediction of archaea was carried out using PICRUSt2, with visualization accomplished in R.

3 Results

3.1 Physicochemical indexes of sediment samples

The physicochemical properties of sediment samples, including salinity, pH, total organic carbon (TOC), total carbon (TC), total nitrogen (TN), carbon/nitrogen (C/N) ratio, and total phosphorus (TP), were assessed in this study across different locations, depths, and seasons (Table 1). During the dry season, NM sediment had a significantly higher pH than ARM sediment, with the exception of the 0–5 cm depth where ARM sediment had a higher pH. Salinity was significantly higher in NM sediment in the 0–10 cm depth, while higher salinity was observed in ARM sediment in the 0–5 cm and 10–15 cm depths during the wet season. Sediment nutrients, including TOC, TC, TN, and TP, were predominantly higher in NM compared to ARM at most depths ($P < 0.05$), regardless of the season. The C/N ratio was higher in NM sediment in the 0–5 cm and 5–10 cm depths during the dry season, while ARM sediment had a higher C/N ratio in the 5–10 cm and 15–20 cm depths during the wet season ($P < 0.05$). The TP concentration was significantly higher in NM sediment in the 0–5 cm depth during the dry season and mostly higher in ARM sediment than in NM sediment at most depths in both seasons. Regarding the vertical distribution of physicochemical properties, sediment pH decreased significantly with depth during the dry season, except for a higher pH in the middle and lower layers during the wet season. Salinity and pH presented a similar distribution pattern. Generally, TOC, TC, TN, C/N, and TP were higher in ARM sediment in the subsurface layer (10–20 cm) in both seasons, while being more concentrated in the surface layer (0–10 cm) in NM. Additionally, the C/N ratio was higher in the middle and lower layers of the sediments.

3.2 Abundance of archaeal 16S rRNA gene

To obtain a quantitative measure of the archaeal community, the abundance of archaeal 16S rRNA gene was detected using qPCR. The abundance of archaeal 16S rRNA gene ranged from 2.60×10^7 to 6.67×10^7 16S rRNA gene copies per gram sediment (wet weight) in NM, while ranging from 1.16×10^7 to 3.90×10^7 copies per gram sediment (wet weight) in ARM (Figure 2). The archaeal abundance was significantly higher ($P < 0.05$) in NM compared to ARM in both wet and dry seasons based on unpaired *t*-test analysis. Although the ANOVA analysis showed no significant differences among different depths ($P > 0.05$), there was a trend in archaeal abundance with increasing depth in NM, followed by a decrease at deeper depths in both seasons. In ARM sediment, archaeal abundance decreased from the surface layer (0–5 cm) to the middle layer (5–10 cm), then slightly increased at deeper depths during the wet season, with a similar trend observed in the dry season.

3.3 Analysis of archaeal alpha diversity

After filtering out ASVs with relative abundance less than 0.001%, a total of 2,091,250 reads were obtained, comprising 2,291 ASVs. The 5–10 cm sediment from NM-Wet had the highest ASV numbers and Chao1 index (1087 ± 95; 1090.85 ± 95.79), while the highest Shannon index was found in the 15–20 cm sediment from ARM-Dry (8.70 ± 0.04). The lowest ASVs, Chao1 index, and Shannon index were detected in the 0–5 cm sediment from NM-Dry (414 ± 62; 414.44 ± 61.63; 6.88 ± 0.14) (Table 2). All samples had a coverage exceeding 99.95%, and the rarefaction curves gradually plateaued, indicating that the sequencing depth in this study provided sufficient information on the vast majority of species within the samples (Table 2; Supplementary Figure S1). Comparing different sites, the ASVs and Chao1 index of sediment archaea in NM significantly increased in the wet season compared to ARM ($P < 0.001$), while the Shannon index of sediment archaea in ARM during the dry season was significantly higher than that in NM ($P < 0.05$). Concerning different depths, the ASVs, Chao1 index, and Shannon index in the 0–5 cm layer showed a significant reduction compared to other depths in both dry and wet seasons ($P < 0.01$) (Supplementary Figure S2).

10.3389/fmars.2024.1380801

TABLE 1 Physicochemical properties of the natural and artificially restored mangroves at different sediment depths collected in both the dry and wet seasons.

EF	Site	NM				ARM			
	Depth (cm)	0–5	5–10	10–15	15–20	0–5	5–10	10–15	15–20
pH	Dry	**6.28 ± 0.00^{a}**	**6.00 ± 0.00^{b}**	**5.78 ± 0.01^{c}**	**5.78 ± 0.00^{c}**	**6.37 ± 0.04^{a}**	**5.81 ± 0.02^{b}**	**5.76 ± 0.01^{b}**	**5.50 ± 0.02^{c}**
	Wet	**6.60 ± 0.03^{c}**	6.80 ± 0.01^{a}	**6.74 ± 0.04^{ab}**	**6.71 ± 0.02^{b}**	**6.70 ± 0.03^{c}**	6.90 ± 0.04^{a}	**6.93 ± 0.02^{ab}**	**6.82 ± 0.02^{b}**
Salinity (g/kg)	Dry	**1.90 ± 0.04^{a}**	**1.63 ± 0.05^{b}**	1.41 ± 0.02^{c}	1.26 ± 0.05^{d}	**1.52 ± 0.05^{a}**	**1.20 ± 0.01^{b}**	1.40 ± 0.04^{a}	1.28 ± 0.05^{ab}
	Wet	**1.25 ± 0.04^{b}**	**1.63 ± 0.05^{a}**	**1.61 ± 0.02^{a}**	1.58 ± 0.02^{a}	**1.61 ± 0.06^{b}**	**1.21 ± 0.02^{c}**	**1.80 ± 0.04^{a}**	1.70 ± 0.07^{ab}
TOC (g/kg)	Dry	**36.63 ± 0.79^{a}**	**35.03 ± 0.88^{a}**	**28.36 ± 0.83^{b}**	**25.88 ± 1.05^{c}**	**17.10 ± 0.40^{c}**	**16.06 ± 0.25^{d}**	**18.73 ± 0.6^{b}**	**22.84 ± 0.46^{a}**
	Wet	**32.96 ± 0.62^{b}**	**27.71 ± 1.28^{c}**	**34.02 ± 0.66^{a}**	**26.49 ± 0.68^{c}**	**20.56 ± 0.31^{b}**	**20.00 ± 0.42^{b}**	**19.35 ± 0.17^{c}**	**22.44 ± 0.32^{a}**
TC (g/kg)	Dry	**38.36 ± 0.59^{a}**	**36.55 ± 0.17^{b}**	**31.40 ± 0.40^{c}**	28.70 ± 0.68^{d}	**19.46 ± 0.12^{b}**	**19.16 ± 0.49^{b}**	**21.05 ± 0.66^{b}**	26.79 ± 0.81^{a}
	Wet	**34.18 ± 0.64^{b}**	**29.12 ± 0.48^{c}**	**36.8 ± 0.13^{a}**	**27.76 ± 0.19^{d}**	**21.42 ± 0.38^{b}**	**21.05 ± 0.42^{b}**	**20.24 ± 0.35^{b}**	**23.79 ± 0.47^{a}**
TN (g/kg)	Dry	**1.80 ± 0.00^{a}**	**1.62 ± 0.01^{b}**	**1.32 ± 0.00^{c}**	**1.16 ± 0.00^{d}**	**0.92 ± 0.01^{b}**	**1.00 ± 0.02^{b}**	**0.94 ± 0.03^{b}**	**1.09 ± 0.01^{a}**
	Wet	**1.72 ± 0.02^{a}**	**1.49 ± 0.01^{b}**	**1.66 ± 0.05^{a}**	**1.39 ± 0.01^{c}**	**1.02 ± 0.02^{a}**	**0.96 ± 0.01^{b}**	**0.89 ± 0.02^{c}**	**0.86 ± 0.01^{c}**
C/N ratio	Dry	**24.84 ± 0.01^{c}**	**26.37 ± 0.01^{b}**	27.65 ± 0.01^{ab}	28.95 ± 0.01^{a}	**24.70 ± 0.02^{b}**	**22.38 ± 0.02^{b}**	26.15 ± 0.01^{ab}	28.74 ± 0.01^{a}
	Wet	23.23 ± 0.02^{b}	**22.76 ± 0.01^{b}**	25.83 ± 0.00^{a}	**23.33 ± 0.01^{b}**	24.44 ± 0.02^{b}	**25.46 ± 0.01^{b}**	26.55 ± 0.02^{b}	**32.35 ± 0.03^{a}**
TP (g/kg)	Dry	**0.42 ± 0.01^{a}**	0.37 ± 0.01^{b}	0.32 ± 0.01^{c}	**0.29 ± 0.01^{c}**	**0.36 ± 0.02^{b}**	0.33 ± 0.02^{b}	0.33 ± 0.01^{b}	**1.07 ± 0.01^{a}**
	Wet	0.36 ± 0.02^{a}	**0.29 ± 0.01^{b}**	0.39 ± 0.00^{a}	**0.30 ± 0.01^{b}**	0.30 ± 0.02^{b}	**0.44 ± 0.01^{a}**	0.35 ± 0.02^{b}	**0.39 ± 0.03^{ab}**

EF, environmental factors; ARM, artificially restored mangroves; NM, natural mangroves. Data represent the mean ± standard deviation from three replicates. Bold data set indicates the significant difference (p-value < 0.05) between ARM and NM in the same depth and season. Different superscript lowercase letters indicate the significant differences (p-value < 0.05) between four different depths in the same season and site.

3.4 Structure and composition of archaeal community

Upon processing, a total of 2,291 ASVs were classified into 12 archaeal phyla, 19 classes, 27 orders, 31 families, and 31 genera. Crenarchaeota was observed as the most abundant archaeal phylum in all samples, with a relative abundance ranging from 51.39% to 78.72%. Other detected archaeal phyla included Thermoplasmatota, Asgardarchaeota, Nanoarchaeota, and Euryarchaeota, with relative abundance ranging from 10.08% to 29.25%, 6.26% to 17.40%, 1.33% to 6.51%, and 0.71% to 2.03%, respectively, across all samples (Supplementary Figure S3). Our annotation identified Bathyarchaeia (51.10%–77.29%) and Nitrososphaeria (0.29%–2.73%) as the most prevalent archaeal classes in the Crenarchaeota phylum. Additionally, Thermoplasmata (10.07%–29.20%) in Thermoplasmatota, Lokiarchaeia (3.54%–5.70%) and Odinarchaeia (0.74%–2.54%) in Asgardarchaeota, Nanoarchaeia (1.33%–6.51%) in Nanoarchaeota, and Thermococci (0.71%–2.03%) in Euryarchaeota were highly abundant in all samples (Figure 3). Within the genera, *norank_c:Bathyarchaeia* exhibited the highest relative abundance across all samples, followed by norank_Marine_Benthic_Group_D, norank_c:Lokiarchaeia, Marine Group III (MG III), and norank_f:SCGC_AAA011_D5 (Supplementary Figure S4).

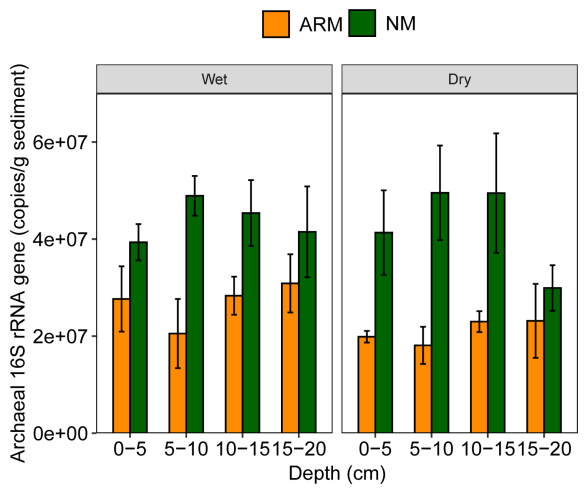

FIGURE 2
Abundance of archaeal 16S rRNA gene in sediment samples of artificially restored mangroves (ARM) and natural mangroves (NM) in wet and dry seasons.

NMDS plots showed that afforestation and sampling depth significantly affected archaeal community structures during both the wet and dry seasons (Figure 4). In the wet season of NM samples, three distinct depth groups were evidently delineated: the first one from depths 0–5 cm, the second one from depths 5–10 cm and 10–15 cm, and the third one from depths 15–20 cm. In the dry season, the 0–5 cm NM sediment samples were distinctly differentiated from the others. However, in the ARM samples, only the depth of 0–5 cm is distinctly differentiated from the rest of the depths in both wet and dry seasons. The ANOSIM tests have confirmed statistically significant differences in the formation of

10.3389/fmars.2024.1380801

TABLE 2 Alpha diversity indicators of the archaeal community in natural and artificially restored mangroves at different sediment depths collected during both the dry and wet seasons.

Sample name	ASV number	Chao1 index	Shannon index	Coverage (%)
Wet_ARM_A	434 ± 121	434.15 ± 121.52	7.29 ± 0.32	100.00
Wet_ARM_B	851 ± 15	853.34 ± 15.45	8.23 ± 0.02	99.98
Wet_ARM_C	809 ± 14	811.49 ± 13.51	8.36 ± 0.02	99.98
Wet_ARM_D	809 ± 61	811.54 ± 61.44	8.35 ± 0.05	99.98
Wet_NM_A	805 ± 124	805.41 ± 124.27	7.52 ± 0.37	99.99
Wet_NM_B	1087 ± 95	1090.85 ± 95.79	8.34 ± 0.13	99.99
Wet_NM_C	1071 ± 45	1073.30 ± 45.55	8.25 ± 0.11	99.98
Wet_NM_D	1024 ± 20	1027.88 ± 19.41	8.45 ± 0.04	99.98
Dry_ARM_A	602 ± 116	603.67 ± 116.54	7.88 ± 0.28	99.99
Dry_ARM_B	945 ± 16	947.90 ± 16.68	8.50 ± 0.05	99.98
Dry_ARM_C	828 ± 76	829.45 ± 75.25	8.39 ± 0.09	99.98
Dry_ARM_D	994 ± 39	1000.93 ± 39.58	8.70 ± 0.04	99.96
Dry_NM_A	414 ± 62	414.44 ± 61.63	6.88 ± 0.14	99.99
Dry_NM_B	774 ± 26	776.78 ± 27.51	7.97 ± 0.05	99.98
Dry_NM_C	799 ± 12	802.66 ± 12.38	8.23 ± 0.02	99.97
Dry_NM_D	842 ± 49	844.47 ± 47.64	8.31 ± 0.05	99.98

Wet, The wet season; ARM, Artificially restored mangroves; NM, Natural mangroves; A, 0–5 cm; B, 5–10 cm; C, 10–15 cm; D, 15–20 cm.

distinct archaeal communities in the sediments of different sites and sampling depths ($P < 0.01$). Furthermore, during the wet season, ANOSIM test indicated that the influence of sampling sites on archaea beta diversity was greater than that of depth (Table 3). In contrast, during the dry season, depth exerted a stronger influence than sampling sites (Table 3).

Using STAMP v2.1.3, we detected differences in the relative abundance of dominant archaeal communities between ARM and NM (Figure 5). During the wet season, Nitrososphaeria and Candidatus *Nitrosopumilus* were found to be significantly more abundant in NM compared to ARM ($P < 0.05$). Furthermore, in both seasons, we observed higher relative abundance of Crenarchaeota, Bathyarchaeia, and *norank_c:Bathyarchaeia* in NM compared to ARM ($P < 0.05$). Conversely, we observed higher abundance of Thermoplasmatota, Thermoplasmata, and MG III in ARM during both seasons ($P < 0.05$).

When looking at different depths, we found that the relative abundance of Crenarchaeota, Bathyarchaeia were significantly higher in the surface layer (0–5 cm) than that in the middle-lower layer (5–20 cm), while Thermoplasmatota exhibited a higher relative abundance in the middle layer (5–20 cm) (Supplementary Table S1).

In terms of different seasons, in ARM sediments, archaeal groups from Asgardarchaeota (phylum) to norank_c:Lokiarchaeia (order) and Odinarchaeia (class) to norank_c:Odinarchaeia (order) were enriched in the dry season (Supplementary Figure S5A). Conversely, Nanoarchaeota groups, MG III were more enriched in the wet season (Supplementary Figure S5A). Archaea in NM sediments also showed that Nanoarchaeota groups were more enriched in the wet season (Supplementary Figure S5B).

3.5 Co-occurrence networks of the archaeal communities

The co-occurrence network graphs of archaea were constructed by ASVs with relative abundance exceeding 0.05% (Figure 6). Each node in the network represented a phylum level, with different phyla being assigned distinct colors. Network analysis of the four graphs revealed that Crenarchaeota, Thermoplasmatota, and Asgardarchaeota were the most abundant phyla in terms of the proportion of nodes in the

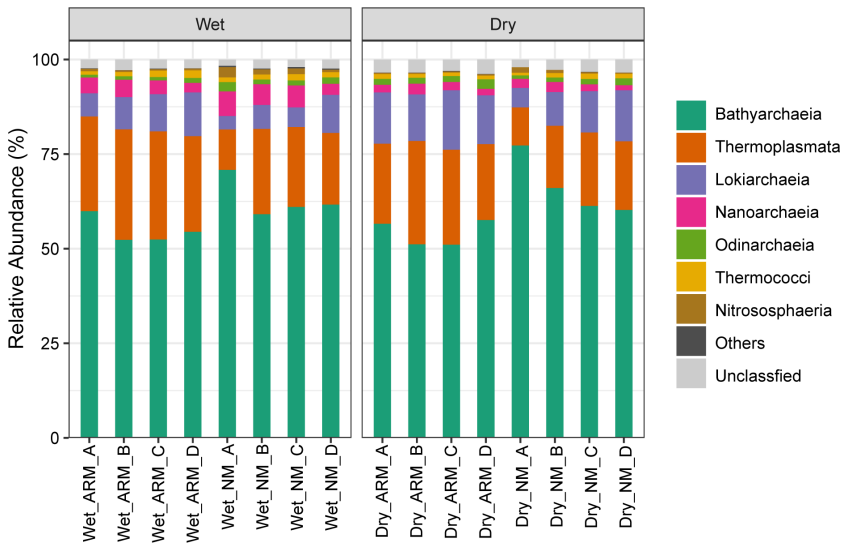

FIGURE 3
Relative abundance of archaea at the class level in Tieshan Bay mangrove sediment in wet and dry seasons.

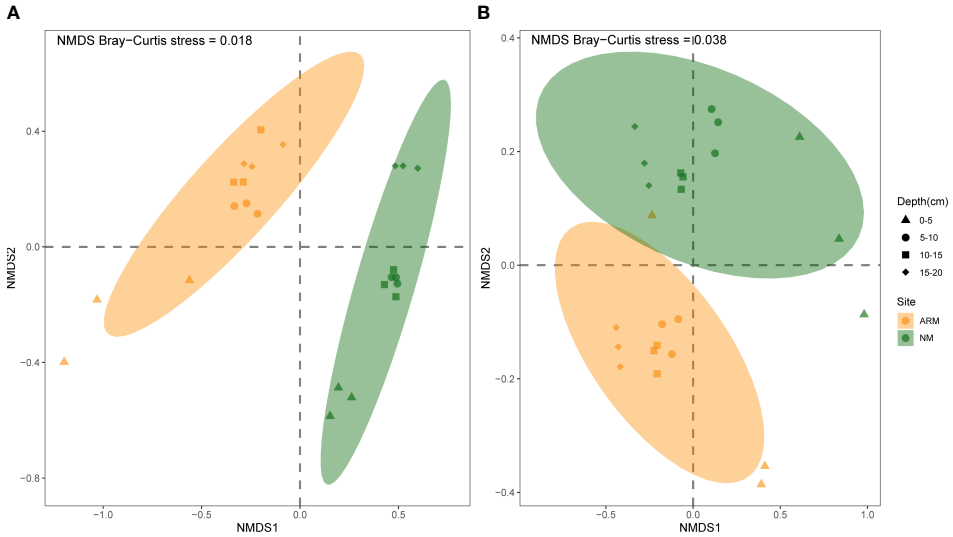

FIGURE 4
NMDS of the compositions of the sediment archaeal communities in the wet **(A)** and dry **(B)** seasons.

network, and this finding was consistent with their high relative abundance observed in the archaeal community composition.

During the wet season, the archaeal network in ARM sediment featured 292 nodes and 4,515 edges, with an average degree of 30.925, while in NM sediment, the archaeal network consisted of 309 nodes, 6,807 edges, and an average degree of 44.058. In the dry season, the ARM sediment's archaeal network contained 176 nodes, 245 edges, and an average degree of 2.800, whereas the NM sediment's archaeal network comprised 316 nodes, 9,863 edges, and an average degree of 62.622 (Table 4). In both seasons, the archaeal network of NM sediment displayed a larger total number of nodes, total number of edges, and average degree compared to ARM sediment, indicating that the NM sediment's archaeal network was more tightly connected and more complex. It's worth noting that all four archaeal networks exhibited positive correlation edges exceeding 90%, suggesting a prevalent coexistence of archaeal species in both ARM and NM sediments (Table 4).

3.6 Relationships between archaeal communities and environmental factors

The RDA biplot indicated that during the wet season, axis 1 and axis 2 explained 40.3% and 21.46% of the variance among the archaea, while during the dry season, they explained 34.03% and 22.13% of the variance, respectively (Figure 7). A Monte Carlo permutations test (n = 999) confirmed that this differentiation was statistically significant ($P = 0.001$). During the wet season, C/N showed the strongest contribution to the species-environment relationship ($r^2 = 0.85$, $P = 0.001$), followed by TN ($r^2 = 0.83$, $P = 0.001$), TOC ($r^2 = 0.74$, $P = 0.001$), TC ($r^2 = 0.73$, $P = 0.001$), and pH ($r^2 = 0.57$, $P = 0.001$). TP ($r^2 = 0.30$, $P = 0.025$) and salinity ($r^2 = 0.17$, $P = 0.155$) contributed less, with salinity having no significant effect on the archaeal community (Supplementary Table S2). During the dry season, pH emerged as the primary driver of the relationship between sediment archaea and environmental factors ($r^2 = 0.74$, $P = 0.001$), followed by C/N ($r^2 = 0.61$, $P = 0.001$), TC ($r^2 = 0.38$, $P = 0.007$), TOC ($r^2 = 0.37$, $P = 0.004$), and TP ($r^2 = 0.34$, $P = 0.014$). Salinity ($r^2 = 0.30$, $P = 0.021$) and TN ($r^2 = 0.24$, $P = 0.046$) played comparatively modest roles (Supplementary Table S2).

Both wet and dry seasons showed correlations between environmental factors and primary archaea (relative abundance > 1%) (Supplementary Figures S6, S7). During the wet season, norank_o:Marine_Benthic_Group_D, norank_p:Aenigmarchaeota, and norank_o:SCGC_AB_179_E04 exhibited significant ($P < 0.05$) positive correlations with pH. In contrast, only norank_o:SCGC_AB_179_E04 showed an extremely significant ($P < 0.01$) negative correlation with pH in the dry season without the other two species exhibiting any significant correlation. During the dry season, norank_o:Marine_Benthic_Group_A, norank_c:Deep_Sea_Euryarchaeotic_Group (DSEG), and Methanocorpusculum were significantly ($P < 0.05$) negatively correlated with pH, whereas such correlations were insignificant during the wet season. In addition, during the wet season, Odinarchaeia, norank_c:Odinarchaeia, norank_c:Deep_Sea_Euryarchaeotic_Group (DSEG), norank_o:Marine_Benthic_Group_A (MBGA), and norank_o:SCGC_AB_179_E04 were significantly ($P < 0.05$) negatively correlated with TC, TOC, and TN, with *Methanococcoides* revealing opposite correlations with TC, TOC, and TN. Crenarchaeota, including Nitrososphaeria, Bathyarchaeia, and *norank_c:Bathyarchaeia*,

TABLE 3 ANOSIM analysis of archaeal community dissimilarities across different sampling sites or depths during dry and wet seasons.

Season	Variable	ANOSIM	
		R	*P*
Wet	Site	0.76	**0.001**
Wet	Depth	0.24	**0.004**
Dry	Site	0.37	**0.001**
Dry	Depth	0.39	**0.001**

Significant differences (P<0.05) are highlighted in bold.

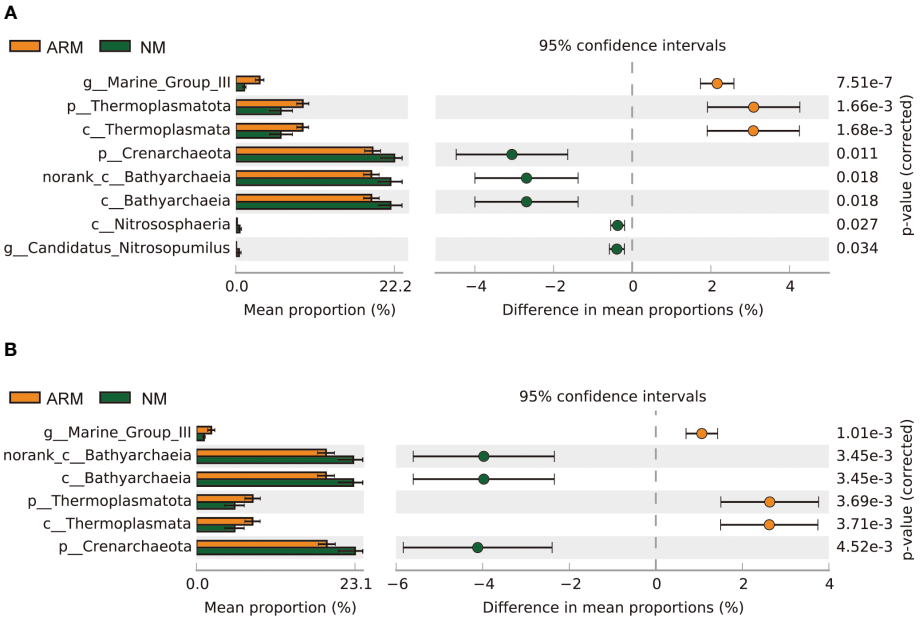

FIGURE 5
Significant differences of sediment primary archaeal community (relative abundance > 0.5%) between ARM and NM in the wet **(A)** and dry **(B)**. The designations "p:" "c:" and "g:" correspond to phylum, class, and genus levels, respectively.

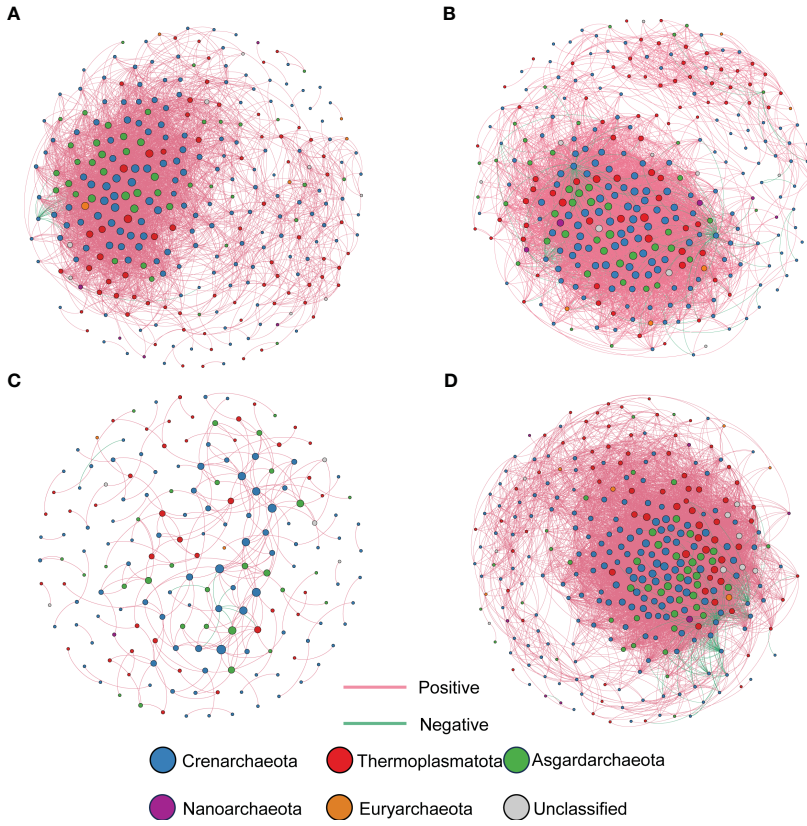

FIGURE 6
Co-occurrence network analysis of archaea communities in sediment from different sites during wet and dry seasons. **(A)** Wet season-artificially restored mangroves; **(B)** Wet season-natural mangroves; **(C)** Dry season-artificially restored mangroves; **(D)** Dry season-natural mangroves. Each node in the network represents an ASV, sized proportionally to its degree, and colored by phylum. Red lines indicate significantly positive correlations (Spearman $r > 0.6$, $P < 0.01$), and green lines indicate significantly negative correlations (Spearman $r < 0.6$, $P < 0.01$).

10.3389/fmars.2024.1380801

TABLE 4 Co-occurrence network topological properties of sediment archaea communities from different sampling positions in dry and wet seasons.

Season	Site	Nodes	Edges	average degree	network diameter	Density	Average path length	Clustering coefficient	Positive correlation (%)
Wet	ARM	292	4515	30.925	10.000	0.106	2.926	0.592	99.47
Wet	NM	309	6807	44.058	9.000	0.143	2.971	0.584	91.39
Dry	ARM	176	245	2.800	11.000	0.016	3.808	0.362	96.73
Dry	NM	316	9863	62.622	8.000	0.199	2.415	0.636	97.52

displayed significant ($P < 0.05$) negative correlations with TC, TOC, and TN. During the dry season, Thermoplasmatota, including Thermoplasmata and MG III, showed a highly significant ($P < 0.01$) positive correlation with TC, TOC, and TN, while norank_o: SCGC_AB_179_E04 indicated significant positive correlations with C/N during both seasons ($P < 0.05$).

3.7 Ecological function prediction of archaea community by PICRUSt2

Using PICRUSt2, function prediction outcomes revealed the potential involvement of archaeal communities in biogenic element processes. In this study, we identified a total of six KEGG first-level metabolic pathways and 45 KEGG second-level metabolic pathways. Among these pathways, 17 KEGG second-level metabolic pathways exhibited a relative abundance greater than 1%, distributed across metabolism, genetic information processes, and environmental information processes (Figure 8). Notably, within the metabolism category, there were 12 second-level functions with relative abundance exceeding 1%, while the genetic information processes had four functions, and the environmental information process had one (Figure 8).

Overall, during the wet season, we observed a higher relative abundance of carbohydrate metabolism and lipid metabolism in natural mangrove sediment compared to artificially restored mangroves, while biosynthesis of other secondary metabolites and nucleotide metabolism exhibited higher activity in artificially restored mangrove sediment (Supplementary Table S3). In the dry season, carbohydrate metabolism, global and overview maps, replication and repair, as well as lipid metabolism demonstrated higher abundance in natural mangroves, whereas metabolism of cofactors and vitamins, biosynthesis of other secondary metabolites, metabolism of terpenoids and polyketides, and signal transduction exhibited relatively higher abundance in artificially restored mangroves (Supplementary Table S4). Certain functions also displayed significant differences in relative abundance at different depths, as detailed in Supplementary Tables S3, S4.

4 Discussion

4.1 The differences between artificially restored mangroves and natural mangroves on the sediment physicochemical properties, archaeal abundance, composition, and community structure

In this study, the concentration of TOC, TC, and TN was consistently higher in natural mangrove sediment during both the

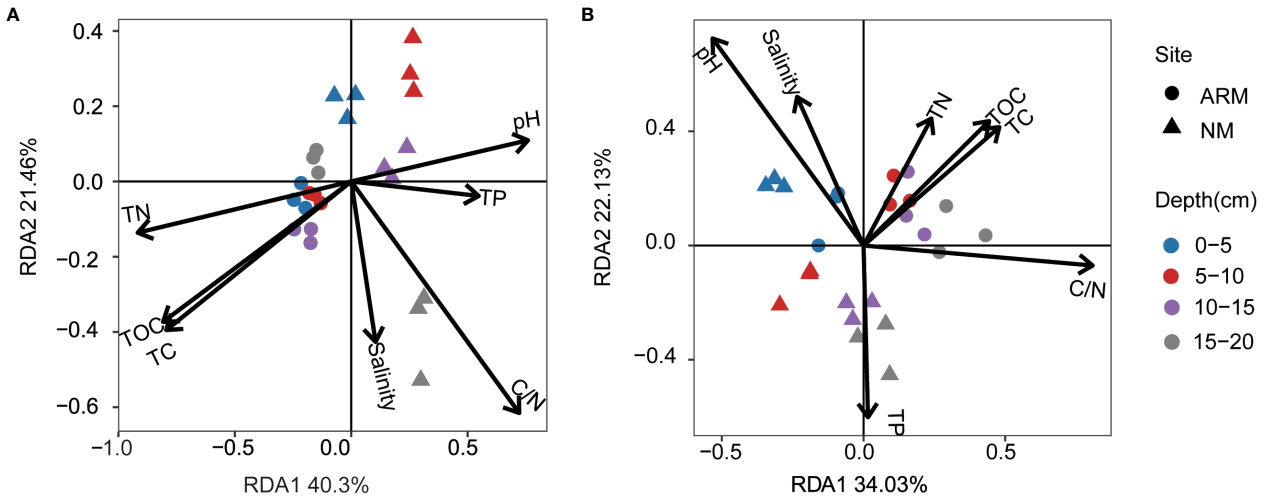

FIGURE 7
RDA analysis of archaea community structure and physicochemical properties in wet **(A)** and dry **(B)** seasons. TC, total carbon; TOC, total organic carbon; TN, total nitrogen; TP, total phosphorus.

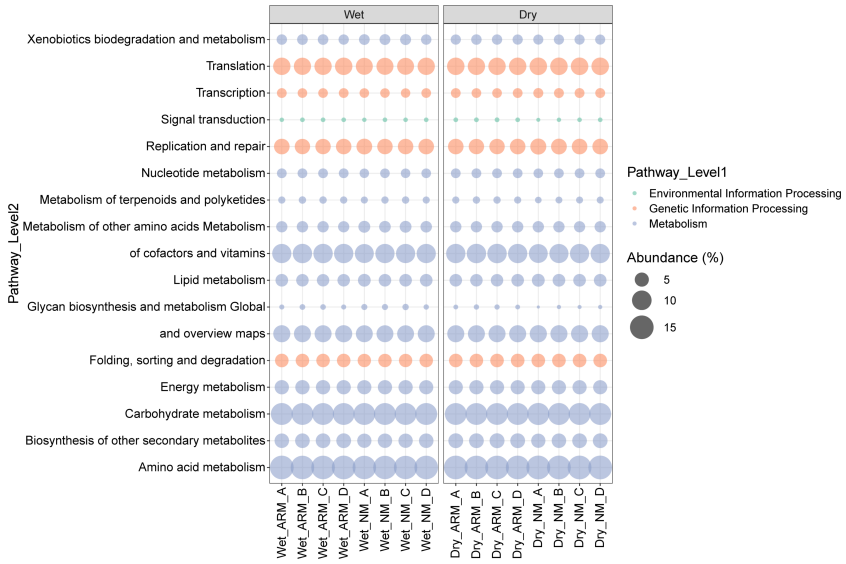

FIGURE 8
Functional prediction of the archaea communities in natural and artificially restored mangrove sediment during dry and wet seasons using PICRUSt2. Bubble colors represent the classification of KEGG level-1 pathways, and the sizes indicate the relative abundance of various KEGG level-2 pathways in different samples. For readability, only functions with relative abundance > 1% are plotted.

dry and wet seasons (Table 1). Previous investigations have indicated that short-term restored mangroves have a lower TC and TN stock (Feng et al., 2017) compared to mature mangroves, which may be due to the high productivity and turnover rates of the soil organic matter in mature mangrove ecosystems (Gao et al., 2019). Although mangrove restoration efforts in the study region commenced in April 2021, with sediment sampling conducted in November 2021 and May 2022, some nutrient levels in the sediment environment had not yet reached their pre-existing levels. The copy numbers of archaeal 16S rRNA genes were consistently higher in natural mangroves compared to artificially restored mangroves (Figure 2). This likely results from mature mangrove ecosystems' long-standing history and more developed ecological environment, which provides a favorable setting for archaea proliferation.

Similar to previous studies (Yan et al., 2006), Crenarchaeota (51.39% to 78.72%) was the predominant archaeal phylum in all sediment samples (Supplementary Figure S3). Crenarchaeota is a stable and specific component of the microbiota in terrestrial habitats and is also the primary community accountable for nitrogen cycling in mangrove ecosystems (Ochsenreiter et al., 2003; Meng et al., 2022). Bathyarchaeia, within Crenarchaeota, and their subordinate genus, Nitrososphaeria, and Candidatus *Nitrosopumilus*, were significantly ($P < 0.05$) more abundant in natural mangroves than in restored mangroves (Figure 5). Bathyarchaeia is now classified in the class Bathyarchaeia within the phylum Crenarchaeota (Romano et al., 2021) and is known for a diverse range of capabilities, such as metabolizing various organic compounds and assimilating inorganic carbon to meet their carbon source and energy requirements (Hou et al., 2023). Nitrososphaeria comprises ammonia-oxidizing archaea (AOA) that are widely distributed in various ecosystems, such as aquatic environments and sediments, fix carbon as chemoautotrophs, and play a crucial role in carbon fixation and contribute significantly to global nitrogen and carbon cycles (Chen et al., 2023). We infer that the high abundance of Bathyarchaeia, Nitrososphaeria, and Candidatus *Nitrosopumilus* in natural mangroves may result from the high TC, TOC, and TN content. Thermoplasmatota (10.08% to 29.25%), Asgardarchaeota (6.26% to 17.40%), Nanoarchaeota (1.33% to 6.51%), and Euryarchaeota (0.71% to 2.03%) were also detected in this study (Supplementary Figure S3). Notably, Euryarchaeota was the dominant phylum in the studied mangroves (Mendes et al., 2012; Zhang et al., 2021). However, the relative abundance of Euryarchaeota was much lower than in other relevant studies. The discrepancies may be attributed to the use of different databases for species annotation. In the NCBI database, the class Thermoplasmata is categorized under the phylum Euryarchaeota (Rinke et al., 2021). However, in the Silva 138 databases used in this study, Thermoplasmata is classified under the phylum Thermoplasmatota. Phylum Thermoplasmatota, class Thermoplasmata, and genus MG III were significantly ($P < 0.05$) more abundant in artificially restored mangroves (Figure 5). MG III was considered as aerobic heterotrophs primarily use proteins and polysaccharides as major energy source (Haro-Moreno et al., 2017). Notably, our findings reveal distinct differences in archaeal community structure between natural and restored mangrove sediments, suggesting that the restoration process significantly influenced these communities. These differential species, such as Bathyarchaeia, Nitrososphaeria, and Thermoplasmata, seem to serve as indicative microorganisms for assessing the mangrove restoration process. In this study, archaeal communities demonstrated similar vertical distribution patterns in natural and artificially restored mangrove sediments, as detailed in Supplementary Table S1. During both the dry and wet seasons, the relative abundance of Crenarchaeota in the surface layer (0–5

cm) was significantly higher than in the middle and lower layers (5–20 cm) in both natural and artificially restored mangrove sediments ($P < 0.05$) (Supplementary Table S1). However, Thermoplasmatota exhibited higher relative abundance in the middle and lower layers (5–20 cm) (Supplementary Table S1), with similar results found in a seagrass meadow (Markovski et al., 2022).

To explore the variations in archaeal potential function across different sites and depths, we predicted functional profiles using PICRUSt2. A higher relative abundance of carbohydrate metabolism and lipid metabolism was observed in natural mangrove may consistent with the proportion of major archaeal groups such as Crenarchaeota and Bathyarchaeia which are more relatively abundant in NM than ARM. Conversely, biosynthesis of other secondary metabolites exhibited relatively higher abundance in artificially restored mangroves. This may due to some archaeal groups might enhance the metabolism of nucleotides and the biosynthesis of other secondary metabolites to adapt to environmental stress. Notably, it's crucial to aware that functional predictions via PICRUSt2 are not a substitute for metagenomic or metatranscriptomic sequencing, as they don't accurately reflect the true abundance of functional genes. Additional research is necessary to ascertain the precision of PICRUSt2 in relation to actual functionality, as opposed to overestimated or underestimated predictions of gene pathways. Nevertheless, our findings could serve as a foundation for subsequent metagenomic or metatranscriptomic investigations into archaeal communities within mangrove sediments.

4.2 Co-occurrence networks of the archaeal communities in artificially restored mangroves and natural mangroves

Microorganisms do not exist in isolation but rather form complex ecosystems of interactions (Faust and Raes, 2012). As such, microbial co-occurrence networks developed from sequencing data are typically used to identify interactions among community members (Berry and Widder, 2014). Positive interactions may result from cross-feeding, mutualism, ecological niche overlap, and other factors, while negative interactions may arise from competitive behavior, predator-prey dynamics, host-parasite relationships, distinct ecological niche preferences, and so on (Faust and Raes, 2012). While co-occurrence networks cannot directly distinguish between these mechanisms (Faust and Raes, 2012), they can aid in deducing potential relationship types based on current associations and offer valuable insights. In the co-occurrence network, the majority of ASVs were found to exhibit positive correlations (as illustrated in Figure 6 and discussed in Table 4). These findings are consistent with previous investigations of archaeal communities in mangrove sediment, which suggest that these communities are more likely to form interactions via synergistic mechanisms rather than antagonistic effects (Chen and Wen, 2021; Zhang et al., 2021). This phenomenon is commonly observed in ecosystems, where many microorganisms rely on interactions like cross-feeding, co-aggregation, co-colonization, or niche overlap to establish ecological relationships (Faust and Raes, 2012; Shi et al., 2019; Chen and Wen, 2021);. Crenarchaeota, Thermoplasmatota, and Asgardarchaeota, which are highly abundant in the archaeal community, were the top three phyla in terms of their proportion in the network nodes. This indicates their significant roles in the network. In both seasons, the archaeal network in natural mangrove sediment had more nodes, connections (edges), an average degree, and density than that of the artificially restored mangrove sediment. This suggests that archaea in natural mangroves were more tightly connected and more complex than their artificially restored counterparts. More complex networks are associated with higher ecological stability (Amato et al., 2019), which supports the notion that the natural mangrove ecosystem was more stable compared to the restored area. However, during the dry season, artificially restored mangroves exhibited an exceptionally sparse archaeal co-occurrence network, which may be attributed to the fact that the sampling took only six months after the commencement of the restoration efforts. Consequently, short-term restoration may not have fostered the development of intricate relational networks among archaea. During the wet season, the archaeal network in artificially restored mangroves became more intricate, although it was still not comparable to the complexity observed in natural mangroves. This illustrates that short-term restoration efforts can enhance ecological stability, but full recovery to its initial state requires an extended period.

4.3 Relationship between archaea and major environmental factors

This study revealed the significant effects of key environmental factors during the wet and dry seasons on the archaeal community structure based on RDA analysis (Figure 7). During the wet season, the C/N ratio emerged as the most significant factor influencing the species-environment relationship (Supplementary Table S2). This ratio served as an indicator of the relative mass of soil organic matter (Lin et al., 2021). Many previous studies have demonstrated the close association between the C/N ratio and the microbial community structure in mangrove ecosystems (Yin et al., 2018; Lin et al., 2021; Huang et al., 2022), thus highlighting the C/N ratio as one of the pivotal environmental variables that shapes microbial community composition within mangrove ecosystems. Moreover, the influence of pH on sediment archaeal community structure was found to be particularly significant during the wet season (Supplementary Table S2). Zhou et al. (2017) identified pH as the primary factor shaping the archaeal community in the Mai Po mangrove sediment. Further research conducted by Qian et al. (2023) demonstrated the significant impacts of pH and acidic volatile sulfides on the depth-dependent distribution of methane, nitrogen, and sulfur cycling genes/pathways within the mangrove sediment. The redox potential is also considered to be one of the significant influencing factors of microbial communities in mangrove sediments (Zhou et al., 2017). In the sediment profile, a vertical transition from sulfate reduction to methanogenesis can be observed with increasing depth, accompanied by a decrease in redox potential

(Euler et al., 2023). In subsequent studies, redox potential should be further incorporated as an environmental factor to be measured.

During the wet season, there were significant negative correlations ($P < 0.05$) between the Odinarchaeia clade, norank_c: Deep_Sea_Euryarchaeotic_Group (DSEG), norank_o: Marine_Benthic_Group_A (MBGA), and norank_o: SCGC_AB_179_E04 with TC, TOC, and TN. Conversely, *Methanococcoides* exhibited significant positive correlations ($P < 0.05$) with TC, TOC, and TN (Supplementary Figure S6). DSEG has been observed in deep-sea sediments (Wang et al., 2010), where it may play a constructive role in cellulose decomposition (Zhao et al., 2018). MBGA, initially discovered in marine sediments, has also been identified in soil environments (Guo et al., 2018) and may possess the ability to thrive in extreme conditions such as high temperatures and high osmotic pressure (Wang et al., 2012). SCGC AB-179-E04 belongs to the class Nitrososphaeria and has been identified in marine sediments (Yang et al., 2022). *Methanococcoides*, a type of methylotrophic methanogens, can utilize methyl compounds such as methanol, methylamine, and methyl sulfides as substrates for methane production (Liu and Whitman, 2008). During the dry season, Nitrososphaeria, Bathyarchaeia, and *norank_c:Bathyarchaeia* displayed significant negative correlations ($P < 0.05$) with TC, TOC, and TN, while Thermoplasmatota, including the class Thermoplasmata and the genus MG III, demonstrated highly significant positive correlations ($P < 0.01$) with TC, TOC, and TN (as shown in Supplementary Figure S7). Bathyarchaeia plays significant ecological roles in the carbon cycling of methane-rich tropical coastal ecosystems (Romano et al., 2021). Recent research has discovered a new order of Thermoplasmatota named "*Candidatus* Yaplasmales", which possesses the capability to anaerobically degrade alkanes, aliphatic hydrocarbons, monocyclic aromatic hydrocarbons, and halogenated organic compounds (Zheng et al., 2022).

5 Conclusions

The archaeal communities in Tieshan Bay's mangrove sediment are primarily made up of Crenarchaeota, Thermoplasmatota, Asgardarchaeota, Nanoarchaeota, and Euryarchaeota. There are notable differences in archaeal abundance and community composition between natural and restored mangrove sediments, with certain taxa, such as Crenarchaeota and Thermoplasmatota, exhibiting significant variations in relative abundance across different sediment depths. Additionally, the C/N ratio contributes the most to the species-environment relationship during the wet season, while pH emerges as the primary driver in the dry season. Furthermore, seasonal differences in the relative abundance of certain archaeal groups (such as Asgardarchaeota, Nanoarchaeota) were observed. Network analysis suggests stronger interconnections among archaeal taxa in natural mangrove habitats compared to artificially restored ones. Moreover, the study reveals that short-term restoration can enhance the development of intricate relational networks among archaea, but has not yet fully restored the ecosystem to its original state. Therefore, this research provides novel empirical data contributing to the restoration and sustainable development of mangroves in Tieshan Bay.

Data availability statement

The original contributions presented in the study are publicly available. This data can be found here: https://www.ncbi.nlm.nih.gov/bioproject/PRJNA1072265/.

Author contributions

ZW: Visualization, Writing – original draft. PZ: Methodology, Validation, Writing – review & editing. YX: Investigation, Project administration, Supervision, Writing – review & editing. TM: Conceptualization, Supervision, Writing – review & editing. YZ: Conceptualization, Supervision, Writing – review & editing.

Funding

The author(s) declare financial support was received for the research, authorship, and/or publication of this article. This study was supported by the National Natural Science Foundation of China (42141016) and Guangxi Science and Technology Base & Talents Fund (GUIKE AD22035968).

Conflict of interest

The authors declare that the research was conducted in the absence of any commercial or financial relationships that could be construed as a potential conflict of interest.

Publisher's note

Supplementary material

The Supplementary Material for this article can be found online at: https://www.frontiersin.org/articles/10.3389/fmars.2024.1380801/full#supplementary-material

References

Alongi, D. M. (2015). The impact of climate change on mangrove forests. *Curr. Clim. Change Rep.* 1, 30–39. doi: 10.1007/s40641-015-0002-x

Amato, P., Besaury, L., Joly, M., Penaud, B., Deguillaume, L., and Delort, A. (2019). Metatranscriptomic exploration of microbial functioning in clouds. *Sci. Rep.* 9, 4383. doi: 10.1038/s41598-019-41032-4

Barbier, E. B., Hacker, S. D., Kennedy, C., Koch, E. W., Stier, A. C., and Silliman, B. R. (2011). The value of estuarine and coastal ecosystem services. *Ecol. Monogr.* 81, 169–193. doi: 10.1890/10-1510.1

Berry, D., and Widder, S. (2014). Deciphering microbial interactions and detecting keystone species with co-occurrence networks. *Front. Microbiol.* 5. doi: 10.3389/fmicb.2014.00219

Bolyen, E., Rideout, J. R., Dillon, M. R., Bokulich, N. A., Abnet, C. C., Al-Ghalith, G. A., et al. (2019). Reproducible, interactive, scalable and extensible microbiome data science using QIIME 2. *Nat. Biotechnol.* 37, 852–857. doi: 10.1038/s41587-019-0209-9

Buelow, C. A., Connolly, R. M., Turschwell, M. P., Adame, M. F., Ahmadia, G. N., Andradi-Brown, D. A., et al. (2022). Ambitious global targets for mangrove and seagrass recovery. *Curr. Biol.* 32, 1641–1649. doi: 10.1016/j.cub.2022.02.013

Callahan, B. J., McMurdie, P. J., Rosen, M. J., Han, A. W., Johnson, A. J. A., and Holmes, S. P. (2016). DADA2: high-resolution sample inference from Illumina amplicon data. *Nat. Methods* 13, 581–583. doi: 10.1038/nmeth.3869

Chen, X., Cai, R., Zhuo, X., Chen, Q., He, C., Sun, J., et al. (2023). Niche differentiation of microbial community shapes vertical distribution of recalcitrant dissolved organic matter in deep-sea sediments. *Environ. Int.* 178, 108080. doi: 10.1016/j.envint.2023.108080

Chen, W., and Wen, D. (2021). Archaeal and bacterial communities assembly and co-occurrence networks in subtropical mangrove sediments under *Spartina alterniflora* invasion. *Environ. Microbiome.* 16, 10. doi: 10.1186/s40793-021-00377-y

Chen, Z., Xu, S., Qiu, Y., Lin, Z., and Jia, X. (2009). Modeling the effects of fishery management and marine protected areas on the Beibu Gulf using spatial ecosystem simulation. *Fish. Res.* 100, 222–229. doi: 10.1016/j.fishres.2009.08.001

Cho, J. C., Lee, D. H., Cho, Y. C., Cho, J. C., and Kim, S. J. (1996). Direct extraction of DNA from soil for amplification of 16S rRNA gene sequences by polymerase chain reaction. *J. Microbiol.* 34, 229–235.

Coolen, M. J. L., Hopmans, E. C., Rijpstra, W. I. C., Muyzer, G., Schouten, S., Volkman, J. K., et al. (2004). Evolution of the methane cycle in Ace Lake (Antarctica) during the Holocene: response of methanogens and methanotrophs to environmental change. *Org. Geochem.* 35, 1151–1167. doi: 10.1016/j.orggeochem.2004.06.009

Dixon, P. (2003). VEGAN, a package of R functions for community ecology. *J. Veg. Sci.* 14, 927–930. doi: 10.1111/j.1654-1103.2003.tb02228.x

Douglas, G. M., Maffei, V. J., Zaneveld, J. R., Yurgel, S. N., Brown, J. R., Taylor, C. M., et al. (2020). PICRUSt2 for prediction of metagenome functions. *Nat. Biotechnol.* 38, 685–688. doi: 10.1038/s41587-020-0548-6

Euler, S., Jeffrey, L. C., Maher, D. T., Johnston, S. G., Sugimoto, R., and Tait, D. R. (2023). Methanogens limited to lower rhizosphere and to an atypical salt marsh niche along a pristine intertidal mangrove continuum. *Limnol. Oceanogr.* 68, 2167–2182. doi: 10.1002/lno.12414

Faust, K., and Raes, J. (2012). Microbial interactions: from networks to models. *Nat. Rev. Microbiol.* 10, 538–550. doi: 10.1038/nrmicro2832

Feng, J., Zhou, J., Wang, L., Cui, X., Ning, C., Wu, H., et al. (2017). Effects of short-term invasion of *Spartina alterniflora* and the subsequent restoration of native mangroves on the soil organic carbon, nitrogen and phosphorus stock. *Chemosphere* 184, 774–783. doi: 10.1016/j.chemosphere.2017.06.060

Fernandes, S. O., Gonsalves, M. J., Nazareth, D. R., Wong, S., Haider, M. N., Ijichi, M., et al. (2022). Seasonal variability in environmental parameters influence bacterial communities in mangrove sediments along an estuarine gradient. *Estuar. Coast. Shelf Sci.* 270, 107791. doi: 10.1016/j.ecss.2022.107791

Friess, D. A., Rogers, K., Lovelock, C. E., Krauss, K. W., Hamilton, S. E., Lee, S. Y., et al. (2019). The state of the world's mangrove forests: past, present, and future. *Annu. Rev. Env. Resour.* 44, 89–115. doi: 10.1146/annurev-environ-101718-033302

Gao, G., Li, P., Zhong, J., Shen, Z., Chen, J., Li, Y., et al. (2019). *Spartina alterniflora* invasion alters soil bacterial communities and enhances soil N_2O emissions by stimulating soil denitrification in mangrove wetland. *Sci. Total Environ.* 653, 231–240. doi: 10.1016/j.scitotenv.2018.10.277

Goldberg, L., Lagomasino, D., Thomas, N., and Fatoyinbo, T. (2020). Global declines in human-driven mangrove loss. *Glob. Change Biol.* 26, 5844–5855. doi: 10.1111/gcb.15275

Guo, W., Xie, W., Li, X., Wang, P., Hu, A., and Zhang, C. (2018). Environmental factors shaping the archaeal community structure and ether lipid distribution in a subtropic river and estuary, China. *Appl. Microbiol. Biot.* 102, 461–474. doi: 10.1007/s00253-017-8595-8

Haro-Moreno, J. M., Rodriguez-Valera, F., López-García, P., Moreira, D., and Martin-Cuadrado, A. (2017). New insights into marine group III Euryarchaeota, from dark to light. *Isme J.* 11, 1102–1117. doi: 10.1038/ismej.2016.188

Hartvigsen, G. (2011). Using R to build and assess network models in biology. *Math. Model. Nat. Pheno.* 6, 61–75. doi: 10.1051/mmnp/20116604

Holguin, G., Vazquez, P., and Bashan, Y. (2001). The role of sediment microorganisms in the productivity, conservation, and rehabilitation of mangrove ecosystems: an overview. *Biol. Fert. Soils.* 33, 265–278. doi: 10.1007/s003740000319

Hou, J., Wang, Y., Zhu, P., Yang, N., Liang, L., Yu, T., et al. (2023). Taxonomic and carbon metabolic diversification of Bathyarchaeia during its coevolution history with early earth surface environment. *Sci. Adv.* 9, eadf5069. doi: 10.1126/sciadv.adf5069

Hu, C., Hu, G., Xu, C., Li, F., and Zhang, Z. (2022). Soil physical and chemical properties effect the soil microbial carbon, nitrogen, and phosphorus stoichiometry in a mangrove forest, South China. *Appl. Ecol. Env. Res.* 20, 4377–4389. doi: 10.15666/aeer/2005_43774389

Hu, M., Sardans, J., Sun, D., Yan, R., Wu, H., Ni, R., et al. (2024). Microbial diversity and keystone species drive soil nutrient cycling and multifunctionality following mangrove restoration. *Environ. Res.* 251, 118715. doi: 10.1016/j.envres.2024.118715

Huang, X., Feng, J., Dong, J., Zhang, J., Yang, Q., Yu, C., et al. (2022). *Spartina alterniflora* invasion and mangrove restoration alter diversity and composition of sediment diazotrophic community. *Appl. Soil Ecol.* 177, 104519. doi: 10.1016/j.apsoil.2022.104519

Huang, Z., Xu, Z., and Chen, C. (2008). Effect of mulching on labile soil organic matter pools, microbial community functional diversity and nitrogen transformations in two hardwood plantations of subtropical Australia. *Appl. Soil Ecol.* 40, 229–239. doi: 10.1016/j.apsoil.2008.04.009

Jacomy, M., Venturini, T., Heymann, S., and Bastian, M. (2014). ForceAtlas2, a continuous graph layout algorithm for handy network visualization designed for the Gephi software. *PLoS One* 9, e98679. doi: 10.1371/journal.pone.0098679

Jia, M., Wang, Z., Mao, D., Ren, C., Song, K., Zhao, C., et al. (2023). Mapping global distribution of mangrove forests at 10-m resolution. *Sci. Bull.* 68, 1306–1316. doi: 10.1016/j.scib.2023.05.004

Li, M., Fang, A., Yu, X., Zhang, K., He, Z., Wang, C., et al. (2021). Microbially-driven sulfur cycling microbial communities in different mangrove sediments. *Chemosphere* 273, 128597. doi: 10.1016/j.chemosphere.2020.128597

Li, M., Ren, L., Zhang, J., Luo, L., Qin, P., Zhou, Y., et al. (2019). Population characteristics and influential factors of nitrogen cycling functional genes in heavy metal contaminated soil remediated by biochar and compost. *Sci. Total Environ.* 651, 2166–2174. doi: 10.1016/j.scitotenv.2018.10.152

Li, Q., Su, L., Yang, T., Zhang, Z., Yu, M., Deng, X., et al. (2022). Prokaryotic community composition in Makran cold seep sediments and the response to environment. *Acta Microbiol. Sin.* 62, 2021–2037. doi: 10.11975/j.issn.1002-6819.2018.03.029

Li, R., Tong, T., Wu, S., Chai, M., and Xie, S. (2019). Multiple factors govern the biogeographic distribution of archaeal community in mangroves across China. *Estuar. Coast. Shelf Sci.* 231, 106414. doi: 10.1016/j.ecss.2019.106414

Lin, G., He, Y., Lu, J., Chen, H., and Feng, J. (2021). Seasonal variations in soil physicochemical properties and microbial community structure influenced by *Spartina alterniflora* invasion and *Kandelia obovata* restoration. *Sci. Total Environ.* 797, 149213. doi: 10.1016/j.scitotenv.2021.149213

Liu, Y., and Whitman, W. B. (2008). Metabolic, phylogenetic, and ecological diversity of the methanogenic archaea. *Ann. N.Y. Acad. Sci.* 1125, 171–189. doi: 10.1196/annals.1419.019

Liu, P., Zhang, H., Song, Z., Huang, Y., and Hu, X. (2021). Seasonal dynamics of Bathyarchaeota-dominated benthic archaeal communities associated with seagrass (*Zostera japonica*) meadows. *J. Mar. Sci. Eng.* 9, 1304. doi: 10.3390/jmse9111304

Lu, K., Yang, Q., Jiang, Y., and Liu, W. (2022). Changes in temporal dynamics and factors influencing the environment of the bacterial community in mangrove rhizosphere sediments in Hainan. *Sustainability* 14, 7415. doi: 10.3390/su14127415

Luis, P., Saint Genis, G., Vallon, L., Bourgeois, C., Bruto, M., Marchand, C., et al. (2019). Contrasted ecological niches shape fungal and prokaryotic community structure in mangroves sediments. *Environ. Microbiol.* 21, 1407–1424. doi: 10.1111/1462-2920.14571

Markovski, M., Najdek, M., Herndl, G. J., and Korlević, M. (2022). Compositional stability of sediment microbial communities during a seagrass meadow decline. *Front. Mar. Sci.* 9. doi: 10.3389/fmars.2022.966070

Mendes, L. W., Taketani, R. G., Navarrete, A. A., and Tsai, S. M. (2012). Shifts in phylogenetic diversity of archaeal communities in mangrove sediments at different sites and depths in southeastern Brazil. *Res. Microbiol.* 163, 366–377. doi: 10.1016/j.resmic.2012.05.005

Meng, S., Peng, T., Liu, X., Pratush, A., Wang, H., Huang, T., et al. (2022). Archaeal communities of South China mangroves and their potential roles in the nitrogen cycle. *Geomicrobiol. J.* 39, 697–704. doi: 10.1080/01490451.2022.2069890

Mescioglu, E., Rahav, E., Belkin, N., Xian, P., Eizenga, J., Vichik, A., et al. (2019). Aerosol microbiome over the Mediterranean Sea diversity and abundance. *Atmosphere* 10, 440. doi: 10.3390/atmos10080440

Mishra, A., Sharma, S. D., and Khan, G. H. (2003). Improvement in physical and chemical properties of sodic soil by 3, 6 and 9 years old plantation of *Eucalyptus tereticornis*: Biorejuvenation of sodic soil. *For. Ecol. Manage.* 184, 115–124. doi: 10.1016/S0378-1127(03)00213-5

Ochsenreiter, T., Selezi, D., Quaiser, A., Bonch Osmolovskaya, L., and Schleper, C. (2003). Diversity and abundance of Crenarchaeota in terrestrial habitats studied by 16S RNA surveys and real time PCR. *Environ. Microbiol.* 5, 787–797. doi: 10.1046/j.1462-2920.2003.00476.x

Offre, P., Spang, A., and Schleper, C. (2013). Archaea in biogeochemical cycles. *Annu. Rev. Microbiol.* 67, 437–457. doi: 10.1146/annurev-micro-092412-155614

Otero, X. L., Lucheta, A. R., Ferreira, T. O., Huerta-Díaz, M. A., and Lambais, M. R. (2014). Archaeal diversity and the extent of iron and manganese pyritization in sediments from a tropical mangrove creek (Cardoso Island, Brazil). *Estuar. Coast. Shelf Sci.* 146, 1–13. doi: 10.1016/j.ecss.2014.05.002

Parks, D. H., Tyson, G. W., Hugenholtz, P., and Beiko, R. G. (2014). STAMP: statistical analysis of taxonomic and functional profiles. *Bioinformatics* 30, 3123–3124. doi: 10.1093/bioinformatics/btu494

Pruesse, E., Peplies, J., and Glöckner, F. O. (2012). SINA: accurate high-throughput multiple sequence alignment of ribosomal RNA genes. *Bioinformatics* 28, 1823–1829. doi: 10.1093/bioinformatics/bts252

Qian, L., Yu, X., Gu, H., Liu, F., Fan, Y., Wang, C., et al. (2023). Vertically stratified methane, nitrogen and sulphur cycling and coupling mechanisms in mangrove sediment microbiomes. *Microbiome* 11, 71. doi: 10.1186/s40168-023-01501-5

Reef, R., Feller, I. C., and Lovelock, C. E. (2010). Nutrition of mangroves. *Tree Physiol.* 30, 1148–1160. doi: 10.1093/treephys/tpq048

Rinke, C., ChuvoChina, M., Mussig, A. J., Chaumeil, P., Davín, A. A., Waite, D. W., et al. (2021). A standardized archaeal taxonomy for the genome taxonomy database. *Nat. Microbiol.* 6, 946–959. doi: 10.1038/s41564-021-00918-8

Romano, R. G., Bendia, A. G., Moreira, J. C. F., Franco, D. C., Signori, C. N., Yu, T., et al. (2021). Bathyarchaeia occurrence in rich methane sediments from a Brazilian ría. *Estuar. Coast. Shelf Sci.* 263, 107631. doi: 10.1016/j.ecss.2021.107631

Shi, Y., Fan, K., Li, Y., Yang, T., He, J. S., and Chu, H. (2019). Archaea enhance the robustness of microbial co-occurrence networks in Tibetan Plateau soils. *Soil Sci. Soc Am. J.* 83, 1093–1099. doi: 10.2136/sssaj2018.11.0426

Sun, D., Huang, Y., Wang, Z., Tang, X., Ye, W., Cao, H., et al. (2024). Soil microbial community structure, function and network along a mangrove forest restoration chronosequence. *Sci. Total Environ.* 913, 169704. doi: 10.1016/j.scitotenv.2023.169704

Tran, H., Wang, H., Hsu, T., Sarkar, R., Huang, C., and Chiang, T. (2019). Revegetation on abandoned salt ponds relieves the seasonal fluctuation of soil microbiomes. *BMC Genom.* 20, 478. doi: 10.1186/s12864-019-5875-y

Valiela, I., Bowen, J. L., and York, J. K. (2001). Mangrove forests: one of the world's threatened major tropical environments. *BioScience* 51, 807. doi: 10.1641/0006-3568(2001)051[0807:MFOOTW]2.0.CO;2

Wang, Y., Feng, Y., Ma, X., and Gu, J. (2013). Seasonal dynamics of ammonia/ammonium-oxidizing prokaryotes in oxic and anoxic wetland sediments of subtropical coastal mangrove mangroves. *Appl. Microbiol. Biot.* 97, 7919–7934. doi: 10.1007/s00253-012-4510-5

Wang, F., Sarengaowa,, Li, T., Ma, X., and Yu, X. (2010). Vertical distribution of archaeal diversity in surface sediment from the Western Pacific Ocean. *Acta Geol. Sin.* 84, 1105–1111. doi: 10.19762/j.cnki.dizhixuebao.2010.08.003

Wang, J., Xu, X., Zhou, L., Tao, S., Liu, X., and Shi, G. (2012). A preliminary study of microbial diversity of the surface layer sediments from the East China Sea. *Oceanol. Limnol. Sin.* 43, 805–813. doi: 10.11693/hyhz201204018018

Yan, B., Hong, K., and Yu, Z. (2006). Archaeal communities in mangrove soil characterized by 16S rRNA gene clones. *J. Microbiol.* 44, 566–571.

Yang, N., Tian, C., Lv, Y., Hou, J., Yang, Z., Xiao, X., et al. (2022). Novel primers for 16S rRNA gene-based archaeal and bacterial community analysis in oceanic trench sediments. *Appl. Microbiol. Biot.* 106, 2795–2809. doi: 10.1007/s00253-022-11893-3

Yin, P., Yin, M., Cai, Z., Wu, G., Lin, G., and Zhou, J. (2018). Structural inflexibility of the rhizosphere microbiome in mangrove plant *Kandelia obovata* under elevated CO_2. *Mar. Environ. Res.* 140, 422–432. doi: 10.1016/j.marenvres.2018.07.013

Zhang, C., Chen, Y., Sun, Y., Pan, J., Cai, M., and Li, M. (2021). Diversity, metabolism and cultivation of archaea in mangrove ecosystems. *Mar. Life Sci. Tech.* 3, 252–262. doi: 10.1007/s42995-020-00081-9

Zhang, X., Hu, B. X., Ren, H., and Zhang, J. (2018). Composition and functional diversity of microbial community across a mangrove-inhabited mudflat as revealed by 16S rDNA gene sequences. *Sci. Total Environ.* 633, 518–528. doi: 10.1016/j.scitotenv.2018.03.158

Zhang, Z., Pan, J., Pan, Y., and Li, M. (2021). Biogeography, assembly patterns, driving factors, and interactions of archaeal community in mangrove sediments. *Msystems* 6, e01381–e01320. doi: 10.1128/mSystems.01381-20

Zhao, H., Yan, B., Xu, Y., Mo, S., Nie, S., Ou, Q., et al. (2020). Spatiotemporal analysis of microbial community structure in the mangrove sediments in Beibu Gulf. *Genom. Appl. Biol.* 39, 2161–2169. doi: 10.13417/j.gab.039.002161

Zhao, X., Zheng, Z., Cai, Y., Zhao, Y., Luo, K., Cui, Z., et al. (2018). Pretreatment by crude enzymatic liquid from Trichoderma harzianum and *Aspergillus* sp improving methane production performance during anaerobic digestion of straw. *Trans. Chin. Soc Agric. Eng.* 34, 219–226. doi: 10.11975/j.issn.1002-6819.2018.03.029

Zheng, P., Wei, Z., Zhou, Y., Li, Q., Qi, Z., Diao, X., et al. (20222022). Genomic evidence for the recycling of complex organic carbon by novel *Thermoplasmatota* clades in deep-sea sediments. *Msystems* 7, e0007722. doi: 10.1128/msystems.00077-22

Zhou, Z., Meng, H., Liu, Y., Gu, J., and Li, M. (2017). Stratified bacterial and archaeal community in mangrove and intertidal wetland mudflats revealed by high throughput 16S rRNA gene sequencing. *Front. Microbiol.* 8. doi: 10.3389/fmicb.2017.02148